Thermal properties of the pyrochlore, $Y_2Ti_2O_7$

Michel B. Johnson [a,b], David D. James [a], Alex Bourque [a], Hanna A. Dabkowska [c],
Bruce D. Gaulin [d,e], Mary Anne White [a,b,*]

[a] Department of Chemistry, Dalhousie University, Halifax, Nova Scotia, Canada B3H 4J3
[b] Institute for Research in Materials, Dalhousie University, Halifax, Nova Scotia, Canada B3H 1W5
[c] Brockhouse Institute for Materials Research, McMaster University, Hamilton, ON, Canada L8S 4M1
[d] Department of Physics and Astronomy, McMaster University, Hamilton, ON, Canada L8S 4M1
[e] Canadian Institute for Advanced Research, 180 Dundas Street West, Toronto, ON, Canada M5G 1Z8

ABSTRACT

The thermal conductivity and heat capacity of high-purity single crystals of yttrium titanate, $Y_2Ti_2O_7$, have been determined over the temperature range $2\,\mathrm{K} \leqslant T \leqslant 300\,\mathrm{K}$. The experimental heat capacity is in very good agreement with an analysis based on three acoustic modes per unit cell (with the Debye characteristic temperature, θ_D, of ca. 970 K) and an assignment of the remaining 63 optic modes, as well as a correction for $C_p - C_v$. From the integrated heat capacity data, the enthalpy and entropy relative to absolute zero, are, respectively, $H(T = 298.15\,\mathrm{K}) - H_0 = 34.69\,\mathrm{kJ\,mol^{-1}}$ and $S(T = 298.15\,\mathrm{K}) - S_0 = 211.2\,\mathrm{J}$ $\mathrm{K^{-1}\,mol^{-1}}$. The thermal conductivity shows a peak at ca. $\theta_D/50$, characteristic of a highly purified crystal in which the phonon mean free path is about $10\,\mu\mathrm{m}$ in the defect/boundary low-temperature limit. The room-temperature thermal conductivity of $Y_2Ti_2O_7$ is $2.8\,\mathrm{W\,m^{-1}\,K^{-1}}$, close to the calculated theoretical thermal conductivity, $\kappa_{\min}$, for fully coupled phonons at high temperatures.

© 2008 Elsevier Inc. All rights reserved.

1. Introduction

Yttrium titanate, $Y_2Ti_2O_7$, belongs to the family of compounds with the general chemical formula $A_2B_2O_7$, isostructural to the mineral pyrochlore, $(NaCa)(NbTa)O_6F/(OH)$ [1]. Pyrochlores are refractory materials with important properties, including ionic conductivity [2,3], optical nonlinearity [4] and high radiation tolerance [5]. They have many potential applications, including thermal barrier coatings [6], high-permittivity dielectrics [7], solid electrolytes in solid-oxide fuel cells [8], and materials for safe disposal of actinide-containing nuclear waste [9]. Furthermore, pyrochlores have promise as ceramic pigments, given their high melting points ($\sim$1600 °C), high refractive index ($n > 2$), and the ability to accept transition metal dopants [10]. The general pyrochlore structure has high symmetry (Fd-$3m$) and is constituted of vertex-sharing tetrahedra as shown schematically in Fig. 1.

Given the interesting properties of pyrochlores, it is not surprising that their fundamental thermal properties also have attracted attention. Studies include molecular dynamics simulations of the thermal conductivities of a large number of pyrochlores [11], theoretical investigations of structure and

thermal conductivity of $La_2Zr_2O_7$ [12] and experimental determinations of formation enthalpies of titanate pyrochlores [13].

Yttrium titanate, $Y_2Ti_2O_7$, often abbreviated as YTO, is an especially important member of the pyrochlore family. It has both extremely strong electron–phonon interactions and high oxygen vacancy concentrations (the large unit cell [$Z = 8$] of YTO allows some of the oxygen ions to move relatively freely) resulting in low diffusion activation energy [14]. Due to the large number of oxygen vacancies, it can be an n-type semiconductor via doping of the Y^{3+} and Ti^{4+} sites [15] and an increase in conductivity of up to two orders of magnitude can occur on doping [16]. The fact that $Y_2Ti_2O_7$ is diamagnetic makes it one of the most amenable pyrochlores for detailed examination, especially by NMR [15]. As the first reported pyrochlore to split water into H_2 and O_2 under UV irradiation, $Y_2Ti_2O_7$ with excess Y has potential as a photocatalyst [17]. $Y_2Ti_2O_7$ also shows promise as a buffer layer on superconductor substrates [18]. A recent theoretical study of the structure and bonding properties of $Y_2Ti_2O_7$ has shown it to be a good candidate for a hard material due to short inter-atomic distances between ions causing the Ti–O and Y–O bonds to have covalent character [19].

Considering the interest in pyrochlores, and the special importance of $Y_2Ti_2O_7$, we have selected this pyrochlore for a detailed experimental investigation of thermal properties. In the present work, the thermal conductivity and heat capacity of $Y_2Ti_2O_7$ have been determined over a wide temperature range (2–300 K), and the contributions of the various degrees of freedom

* Corresponding author at: Department of Chemistry, Dalhousie University, Halifax, Nova Scotia, Canada B3H 4J3. Fax: +1 902 494 1310.
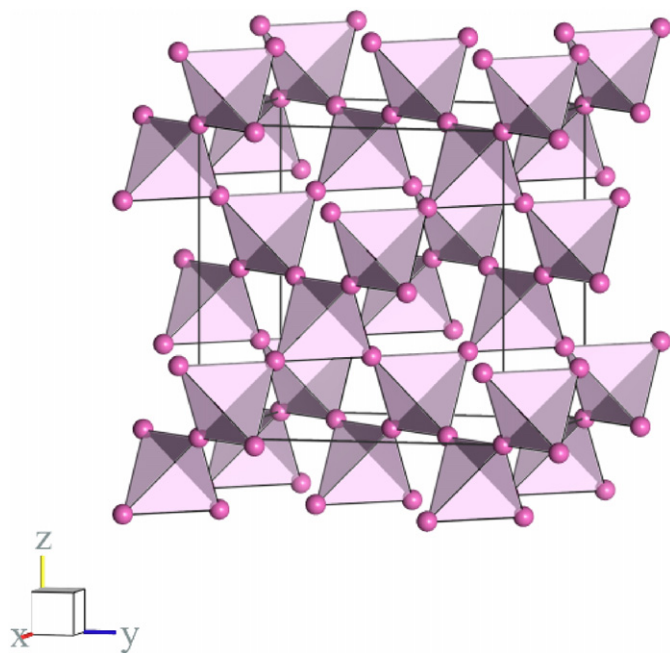E-mail address: mary.anne.white@dal.ca (M.A. White).

Fig. 1. A general view of the pyrochlore structure, showing the linked polyhedra.

to the latter have been assessed. The concomitant advanced understanding concerning the lattice dynamics of $Y_2Ti_2O_7$ provides a firm foundation for analysis of the temperature-dependence of its thermal conductivity and comparison with other pyrochlores.

2. Experimental materials and methods

2.1. Preparation of $Y_2Ti_2O_7$

Several large single crystals of $Y_2Ti_2O_7$ were grown using a two-mirror NEC floating zone image furnace. The details of the crystal growths were similar to those previously reported for single crystal $Tb_2Ti_2O_7$ [20]. The starting materials for the polycrystalline rods were 99.999% pure Y_2O_3 and 99.995% pure TiO_2, both from Alfa Aesar. These materials were pre-annealed at 1273 K, and the resulting rod of $Y_2Ti_2O_7$ was sintered at 1473 K. The final single crystal growth speed in the image furnace was $5\,mm\,h^{-1}$ and the growth was carried out in air. Smaller single crystals, used for the thermal measurements, were cut from the larger crystals. $Y_2Ti_2O_7$ is cubic and the samples were not oriented.

2.2. Thermal measurements

Thermal conductivities (κ) over the temperature range from 2 to 300 K were determined using the thermal transport option of a Physical Property Measurement System (PPMS, by Quantum Design). A two-probe configuration (heater and hot thermometer on one lead; cold foot and cold thermometer on the other) was used and the determination of κ was based on steady-state thermal gradients [21]. A piece of a single crystal of mass 16.77 mg (cross-sectional area: $4.51\,mm^2$; thickness 0.74 mm), polished on both faces, was epoxied (Tra-Duc 2902 from Tra-Con, Inc.) to two disk-shaped gold-plated copper leads. The temperature drop across the sample during measurements was typically $\Delta T \sim 0.03\,T$. Thermal conductivity was measured using step-wise methods.

The maximum heater power was 50 mW. Uncertainty in thermal conductivity measurements is within 5%.

Experimental heat capacities of several pieces of single crystals of $Y_2Ti_2O_7$ cut from larger single crystals and polished on at least one side (for good thermal contact with the tray) were measured over the temperature range from 2 to 300 K using the relaxation calorimetric technique of the PPMS. Four single crystals of various masses (9.93, 16.77 [same sample as for thermal conductivity], 21.10 and 31.65 mg) were measured. In principle, larger samples should give more accurate heat capacity measurements because of their larger contribution to the total heat capacity, but we have found that sometimes large samples give falsely low heat capacity measurements in the PPMS due to long relaxation times [22], so measurement of a range of sample masses is recommended for high accuracy. For $T > 20$ K, these samples contributed in the following proportions to the total heat capacity: from 35% to 55% (9.93 mg sample), or from 65% to 80% (31.65 mg sample). The two-tau method of heat capacity data analysis [23], which allows separately for relaxation of the temperature within the sample and within the addenda, was used. Overall uncertainty in the heat capacity is within 1% in the range $5\,K < T < 300\,K$, and within 5% for $T < 5\,K$ [22].

3. Results and discussion

3.1. Heat capacity of $Y_2Ti_2O_7$

Since the heat capacity provides direct information concerning the lattice dynamics, which is important to the interpretation of the thermal conductivity results, we begin with discussion of the heat capacity results.

The heat capacity of $Y_2Ti_2O_7$ (Fig. 2; full data tables given in the Supplementary Information) is smooth and shows no evidence of phase transitions over the temperature range examined. Furthermore, the data showed no dependence on the sample mass for $T < 70$ K, but at higher temperatures the apparent heat capacity of the most massive sample fell below the other results, indicating inaccuracy due to a thermal lag in the sample during the measurement. In further analysis and discussion presented below, the data for the 31.65 mg sample for $T > 70$ K are omitted.

The low-temperature ($T < 30$ K) heat capacity of a polycrystalline sample of $Y_2Ti_2O_7$ has been reported recently [24] and is in good agreement with the present data in the temperature range of overlap. One advantage of the wider temperature range here is further quantification of the chemical thermodynamics of
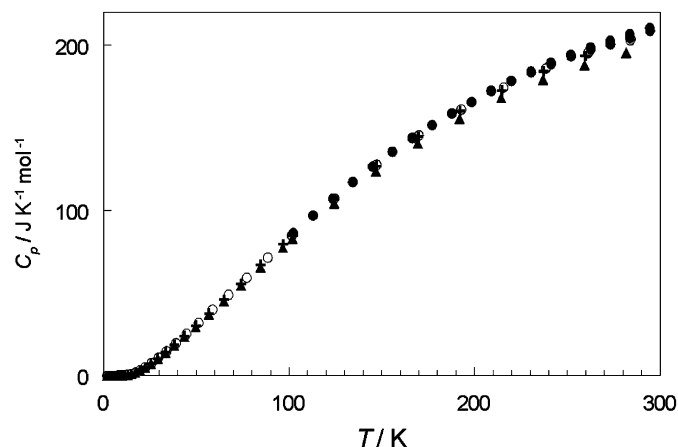

Fig. 2. Heat capacity of $Y_2Ti_2O_7$ as a function of temperature. Sample mass: +, 9.93 mg; ●, 16.7 mg; ○, 21.10 mg and ▲, 31.65 mg.

pyrochlores. We integrated the experimental heat capacity of $Y_2Ti_2O_7$ to assess the enthalpy and entropy relative to absolute zero and find, respectively, $H(T = 298.15\,K) - H_0 = 34.69\,kJ\,mol^{-1}$ and $S(T = 298.15\,K) - S_0 = 211.2\,J\,K^{-1}\,mol^{-1}$. A complete tabulation of $C_p(T)$, $H(T) - H_0$ and $S(T) - S_0$ for $Y_2Ti_2O_7$ is given in the deposited information.

Because pyrochlores can have unusual magnetic properties [25], the diamagnetic compound $Y_2Ti_2O_7$ plays an important role in delineation of magnetic contributions to the heat capacity of paramagnetic pyrochlores. In order to check for possible effects of magnetic impurities in our $Y_2Ti_2O_7$ and concomitant effects such as magnetostriction, we also determined the heat capacity of $Y_2Ti_2O_7$ at a magnetic field of 9 T. With the null hypothesis that the heat capacity is independent of field, t-test scores ranged from 0.4 to 0.9, depending on the temperature range. To reject the null hypothesis at $>95\%$ confidence level, a t-test score >2 would be required. Therefore, we have shown that the heat capacity of $Y_2Ti_2O_7$ from $T = 2$ to 300 K is independent of magnetic field up to 9 T. This information implies exceptionally high purity of the $Y_2Ti_2O_7$ sample, as also evidenced by the phonon mean free path analysis (*vide infra*).

A good test of our understanding of the lattice dynamics of $Y_2Ti_2O_7$ is to compare the calculated and experimental heat capacities. The observed molar heat capacity, $C_{p,m}$, of $Y_2Ti_2O_7$ can be considered as the contributions from acoustic modes (C_v(acoustic)), the optic modes (C_v(optic)) and $C_p - C_v$, and we consider each below.

There are no experimental data (e.g., velocity of sound or elastic constants) available for $Y_2Ti_2O_7$ to calculate the Debye characteristic temperature, θ_D, from which the acoustic heat capacity can be assessed. However, the elastic properties of $Y_2Ti_2O_7$ have been calculated from first principles [26], and from this information, we have calculated $\theta_D = 967\,K$. Although there could be some uncertainty associated with this value (perhaps $\pm 50\,K$), this does not detract significantly from the accuracy of our calculated acoustic heat capacity since its contribution is relatively small: with two formula units per unit cell, the acoustic modes contribute only three degrees of freedom per unit cell, compared with 63 for the optic modes. The acoustic heat capacity, C_v(acoustic), calculated using the Debye model, as shown in Fig. 3, contributes only about 4% to the total heat capacity at room temperature.

Some of the frequencies of the optic modes for $Y_2Ti_2O_7$ have been determined experimentally by Raman and IR spectroscopy [27], and conf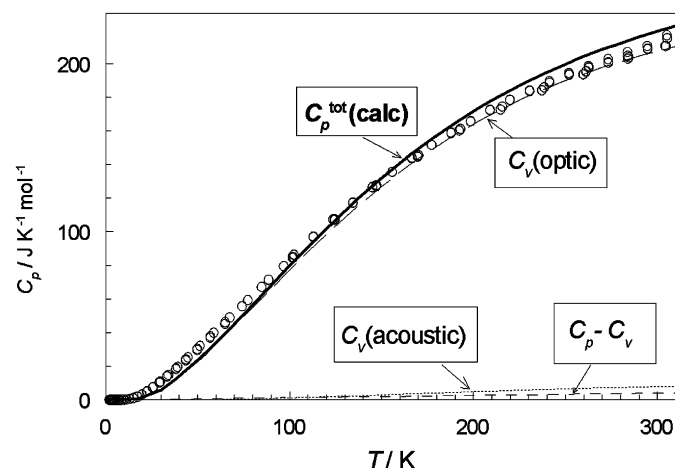irmed theoretically with a short-range force constant model [28]. Although these assignments omit the Raman- and IR-silent modes, the latter have been calculated for $Sm_2Ti_2O_7$, $Gd_2Ti_2O_7$ and $Yb_2Ti_2O_7$ [29] and, on the basis of trends with molecular mass, we have estimated the frequencies of the silent modes of $Y_2Ti_2O_7$. The complete list of frequencies used to calculate the optic contribution to the heat capacity (using the Einstein model) is presented in Table 1 and C_v(optic) is shown in Fig. 3.

The calculations of the optic and acoustic contributions to the heat capacity are for constant volume, but the experimental data are for constant pressure, so we require an additional term, $C_p - C_v$ to compare the calculations with the experiments. The $p - V$ correction can be assessed from

$$C_p - C_v = \frac{\alpha^2 VT}{\beta_T} \tag{1}$$

where α is the thermal expansion coefficient, V the molar volume and β_T the isothermal compressibility. The molar volume is known from single-crystal X-ray diffraction studies [30], and although not all the required additional information is known for calculation of $C_p - C_v$ for $Y_2Ti_2O_7$, the contribution of this term to the total heat capacity is small enough that reasonable estimations do not introduce serious error. In particular, the detailed thermal expansion coefficient for $Y_2Ti_2O_7$ has not been reported, so the thermal expansion coefficient of $Tb_2Ti_2O_7$ [31] was used. (The lattice expansion for $Y_2Ti_2O_7$ at $T = 120\,K$ has been reported [32] and shows this to be a reasonable approximation.) The value of β_T was taken from theoretical studies [26] since experimental data are not available. The contribution of $C_p - C_v$ is shown in Fig. 3.

The total calculated heat capacity, also shown in Fig. 3, provides a good representation of the experimental heat capacity. It is apparent that the optic modes are the main contributor and we have treated them as dispersionless (i.e., used the zone-center values), which might introduce some error. Nevertheless, we can confirm that the assigned lattice dynamics provide an accurate description for $Y_2Ti_2O_7$.

In parallel with the Neuman–Kopp law which indicates that heat capacities can be approximated by the sum of the heat capacities of the constituent atoms, we have shown that for

Fig. 3. Experimental heat capacity of $Y_2Ti_2O_7$ (shown as o), the total calculated heat capacity of $Y_2Ti_2O_7$, C_p^{tot}(calc), and the contributions to the calculated heat capacity.

Table 1
Optic mode assignments for $Y_2Ti_2O_7$, used to calculated C_v(optic).

| Frequency/cm^{-1}	Assignment	Reference
105	F_{1u}	Expt. [27]
176	F_{1u}	Expt. [27]
225	F_{2g}	Expt. [27]
248	F_{1u}	Expt. [27]
285	F_{1u}	Expt. [27]
318	F_{2g}	Expt. [27]
333	E_g	Expt. [27]
410	F_{1u}	Expt. [27]
462	F_{1u}	Expt. [27]
531	F_{2g}	Expt. [27]
527	A_{1g}	Expt. [27]
568	F_{1u}	Expt. [27]
586	F_{2g}	Expt. [27]
110	E_u	Est. from [29]
119	F_{2u}	Est. from [29]
125	A_{2u}	Est. from [29]
159	A_{2u}	Est. from [29]
225	F_{1g}	Est. from [29]
255	E_u	Est. from [29]
285	F_{2u}	Est. from [29]
400	F_{1g}	Est. from [29]
417	E_u	Est. from [29]
458	F_{2u}	Est. from [29]
460	A_{2u}	Est. from [29]
500	F_{2u}	Est. from [29]
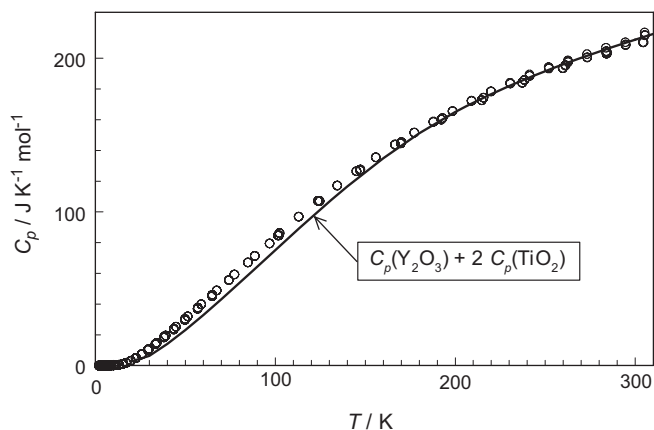
Fig. 4. Comparison of the experimental heat capacity of $Y_2Ti_2O_7$ (o) with the heat capacity calculated from the constituent oxides, $C_p(Y_2O_3)+2\,C_p(TiO_2)$.

inorganic oxides the heat capacity often can be estimated by the sum of the heat capacities of the constituent oxides [33]. Recently, we [34] and others [35] have shown that constituent additivity fails when the complex oxides have additional lattice dynamical features such as low-frequency optic modes associated with movement of complex polyhedra. In Fig. 4, we compare the experimental heat capacity of $Y_2Ti_2O_7$ with the weighted sum of the heat capacities of Y_2O_3 [36] and the rutile form of TiO_2 [37] and find that they match well, indicating no anomalous lattice dynamics in $Y_2Ti_2O_7$.

3.2. Thermal conductivity of $Y_2Ti_2O_7$

The measured thermal conductivity of $Y_2Ti_2O_7$, shown in Fig. 5 (data table in the Supplementary Information), represents a classic case of the thermal conductivity of a highly ordered hard insulator, with a peak at $T\sim\theta_D/50$ in the temperature range where the phonon–phonon collisions become limited by the sample boundaries and/or defects [38]. The room-temperature thermal conductivity can be compared with the minimum theoretical thermal conductivity, κ_{min}, for fully coupled phonons at high temperatures [39]:

$$\kappa_{min} = \frac{k_B n^{2/3}}{2.48}(2v_t + v_l) \qquad (2)$$

where n is the number of atoms per unit volume and v_t and v_l are the transverse and longitudinal sound speeds, respectively. Using the speed of sound [26] as for the heat capacity analysis, gives κ_{min} of $2.4\,W\,m^{-1}\,K^{-1}$, in good agreement with the experimental result, $2.8\,W\,m^{-1}\,K^{-1}$.

The phonon mean free path, λ, can be estimated from the simple Debye model of thermal conductivity:

$$\kappa = \frac{Cv\lambda}{3} \qquad (3)$$

where C is the heat capacity per unit volume and v is the acoustic phonon speed. The temperature-dependence of λ, as shown in Fig. 6, is typical for a highly purified single crystal in which the heat is carried by acoustic phonons that are limited in their mean free path by phonon–phonon collisions at high temperatures (short mean free path) and by low quantities of defects at low temperature (λ at low temperatures of about $10\,\mu m$).

Molecular dynamics simulations of the thermal conductivity of $Y_2Ti_2O_7$ at $T = 1473\,K$ predict a value of $2.6\,W\,m^{-1}\,K^{-1}$[11], not unreasonable in light of the present results. From the perspective of thermal barrier coatings, pyrochlores are thought to be competitive as replacements for yttria-stabilized zirconia, espe-
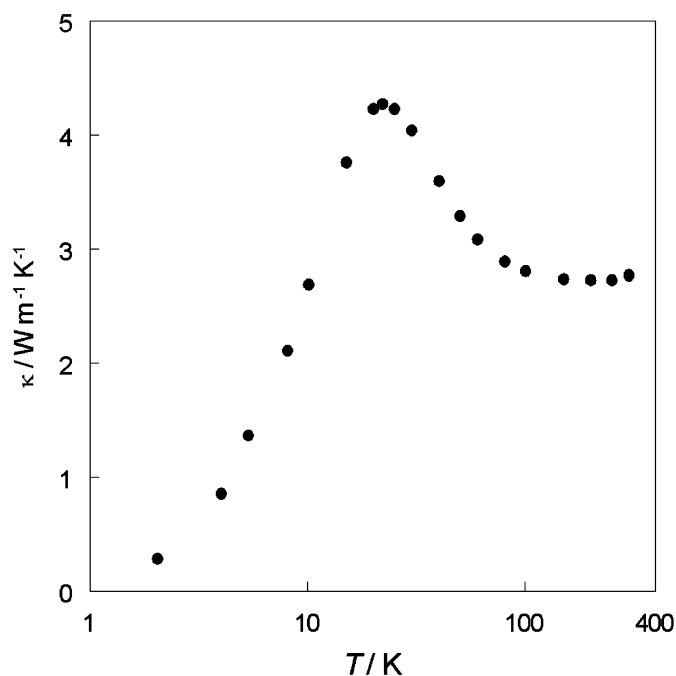

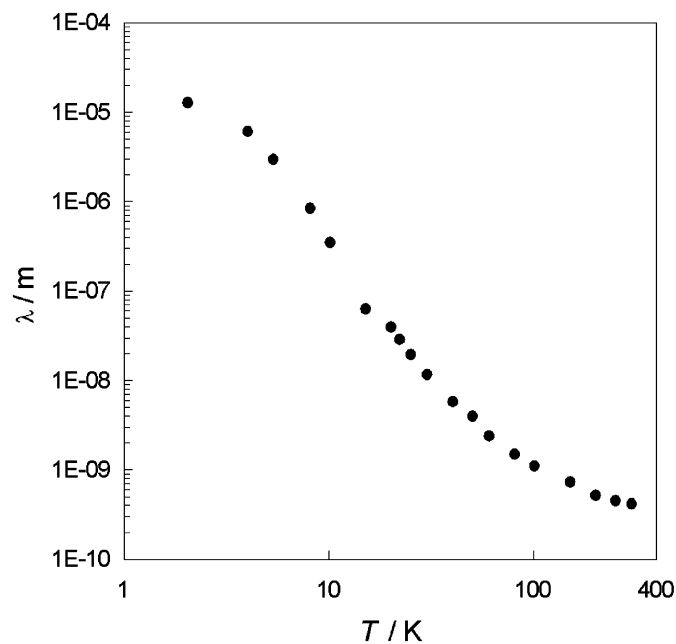**Fig. 5.** Thermal conductivity as a function of temperature for $Y_2Ti_2O_7$.

Fig. 6. Phonon mean free path for $Y_2Ti_2O_7$ as a function of temperature.

cially if the thermal conductivity can be lower than $2–3\,W\,m^{-1}\,K^{-1}$. Our results are for a single crystal of highly purified $Y_2Ti_2O_7$ so the values of κ are maximal, and polycrystallinity, porosity and addition of impurities could lower the thermal conductivity into a useful range for thermal barrier coatings.

Pyrochlores have been suggested as an inert matrix for actinide transmutation, and to efficiently remove heat from matrices with high concentrations of actinides, κ in the range above ca. $2\,W\,m^{-1}\,K^{-1}$ is required [40]. Compared with $Nd_2Zr_2O_7$ and $La_2Zr_2O_7$ ($\kappa\sim1.7\,W\,m^{-1}\,K^{-1}$ [40] and $1.5\,W\,m^{-1}\,K^{-1}$ [41], respectively), our data show that $Y_2Ti_2O_7$ also holds promise for these applications.

Acknowledgments

Appendix A. Supplementary material

Supplementary data associated with this article can be found in the online version at doi:10.1016/j.jssc.2008.12.027.

References

[1] M.A. Subramanian, G. Aramudan, G.V. Subba Rao, Prog. Solid State Chem. 15 (1983) 55.
[2] S.A. Kramer, H.L. Tuller, Solid State Ionics 82 (1995) 15.
[3] T. Norby, J. Mater. Chem. 11 (2001) 11.
[4] F.W. Shi, X.J. Meng, G.S. Wang, T. Lin, J.H. Ma, Y.W. Li, J.H. Chu, Phys. B: Condens. Matter 370 (2005) 277.
[5] G.R. Lumpkin, M. Pruneda, S. Rios, K.L. Smith, K. Trachenko, K.R. Whittle, N.J. Zaluzec, J. Solid State Chem. 180 (2007) 1512.
[6] R. Vassen, D. Sebold, D. Stoever, Ceram. Eng. Sci. Proc. 28 (2008) 27.
[7] W. Ren, S. Trolier-McKinstry, C.A. Randall, T.R. Shrout, J. Appl. Phys. 89 (2001) 767.
[8] B.J. Wuensch, K.W. Eberman, C. Heremans, E.M. Ku, P. Onnerud, E.M. Yeo, S.M. Haile, J.K. Stalick, J.D. Jorgensen, Solid State Ionics 129 (2000) 111.
[9] R.C. Ewing, W.J. Weber, J. Lian, J. Appl. Phys. 95 (2004) 5949.
[10] F. Matteuccci, G. Cruciani, M. Dondi, G. Baldi, A. Barzanti, Acta Materialia 55 (2007) 2229.
[11] P.K. Schelling, S.R. Phillpot, R.W. Grimes, Philos. Mag. Lett. 84 (2004) 127.
[12] B. Liu, J.Y. Wang, Y.C. Zhou, T. Liao, F.Z. Li, Acta Materialia 55 (2007) 2949.
[13] K.B. Helean, S.V. Ushakov, C.E. Brown, A. Navrotsky, J. Lian, R.C. Ewing, J.M. Farmer, L.A. Boatner, J. Solid State Chem. 177 (2004) 1858.
[14] D. Goldschmidt, H.L. Tuller, Phys. Rev. B 34 (1986) 5558.
[15] N. Kim, C.P. Grey, Dalton Trans. (2004) 3048.
[16] S. Kramer, M. Spears, H.L. Tuller, Solid State Ionics 72 (1994) 59.
[17] M. Higashi, R. Abe, K. Sayama, H. Sugihara, Y. Abe, Chem. Lett. 34 (2005) 1122.
[18] H. Lei, Y. Sun, X. Zhu, W. Song, J. Yang, H. Gu, IEEE Trans. Appl. Supercond. 17 (2007) 3819.
[19] R. Terki, G. Bertrand, H. Aourag, C. Coddet, Phys. Rev. B 392 (2006) 341.
[20] J.S. Gardner, B.D. Gaulin, D. McK. Paul, J. Crys. Growth 191 (1998) 740.
[21] O. Maldonado, Cryogenics 32 (1992) 908.
[22] C.A. Kennedy, M. Stancescu, R.A. Marriott, M.A. White, Cryogenics 47 (2007) 107.
[23] J.S. Hwang, K.J. Lin, C. Tien, Rev. Sci. Instrum. 68 (1997) 94.
[24] P. Dasgupta, Y.M. Jana, A. Nag Chattopadhyay, R. Higashinaka, Y. Maeno, D. Ghosh, J. Phys. Chem. Solids 68 (2007) 347.
[25] J.P.C. Ruff, J.P. Clancy, A. Bourque, M.A. White, M. Ramazanoglu, J.S. Gardner, Y. Qiu, J.R.D. Copley, M.B. Johnson, H.A. Dabkowska, B.D. Gaulin, Phys. Rev. Lett. 101 (2008) 147205.
[26] J.M. Pruneda, E. Artacho, Phys. Rev. B 72 (2005) 085107.
[27] M.T. Vandenborre, E. Husson, J.P. Chatry, D. Michel, J. Raman Spectrosc. 14 (1983) 63.
[28] H.C. Gupta, S. Brown, N. Rani, V.B. Gohel, J. Raman Spectrosc. 32 (2001) 41.
[29] H. C. Gupta, Private communication, 2008.
[30] W.J. Becker, G. Will, Z. Kristallogr, Kristallgeom., Kristallphys., Kristallchem. 131 (1970) 278.
[31] S.-W. Han, J.S. Gardner, C.H. Booth, Phys. Rev. B 69 (2004) 024416.
[32] J.P.C. Ruff, B.D. Gaulin, J.P. Castellan, K.C. Rule, J.P. Clancy, J. Rodriguez, H.A. Dabkowska, Phys. Rev. Lett. 99 (2007) 237202.
[33] L. Qiu, M.A. White, J. Chem. Educ. 78 (2001) 1076.
[34] C.A. Kennedy, M.A. White, A.P. Wilkinson, T. Varga, Phys. Rev. B 75 (2007) 224302.
[35] R. Stevens, J. Linford, B.F. Woodfield, J. Boerio-Goates, C. Lind, A.P. Wilkinson, G. Kowach, J. Chem. Thermodyn. 35 (2003) 919.
[36] H.W. Goldstein, E.F. Neilson, P.N. Walsh, D. White, J. Phys. Chem. 63 (1959) 1445.
[37] D. de Ligny, P. Richet, E.F. Westrum Jr., J. Roux, Phys. Chem. Miner. 29 (2002) 267.
[38] M.A. White, Properties of Materials, Oxford University Press, Oxford, 1999.
[39] D.G. Cahill, R.O. Pohl, Ann. Rev. Phys. Chem. 39 (1988) 93.
[40] S. Lutique, R.J.M. Konings, V.V. Rondinella, J. Somers, T. Wiss, J. Alloys Compd. 352 (2003) 1.
[41] R. Vassen, X. Cao, F. Tietz, D. Basu, D. Stöver, J.L. Smialek, J. Am. Ceram. Soc. 83 (2000) 2023.